Proc. Natl. Acad. Sci. USA
Vol. 81, pp. 7088–7092, November 1984
Biophysics

A consistent picture of protein dynamics

(Mössbauer spectroscopy/low-temperature crystallography/intramolecular motion/Brownian diffusion/computer simulations)

F. PARAK* AND E. W. KNAPP†

*Institut für Physikalische Chemie der Universität Münster, D-4400 Münster, Federal Republic of Germany; and †Physik-Department, Technische Universität München, D-8046 Garching, Federal Republic of Germany

Communicated by R. L. Mössbauer, July 16, 1984

ABSTRACT **Information about the protein dynamics of myoglobin obtained by x-ray and Mössbauer investigations is analyzed and compared with computer simulations. Computer simulations give correct amplitudes of mean-square displacements but fail in the description of the time dependence of motions. Our model describes protein dynamics at physiological temperatures as an overdamped diffusion-like motion in a restricted space. The fluctuations occur around the average conformation determined by x-ray structure analysis. The gain in entropy drives the molecule into the transition state and, in this way, accounts for its flexibility.**

In recent years the interest in the flexibility of proteins has increased tremendously. This reflects the fact that many functional properties of these molecules cannot be completely understood from the average structure as determined by x-ray analysis. Reaction rates, for instance, are correlated with dynamic properties (1).

In general, protein flexibility has two major consequences. (*i*) An ensemble of typically 10^{16} protein molecules is necessary for experimental investigation. The individual flexible molecules of such an ensemble will show small structural differences. One can say that molecules that have not one well-defined structure but a number of closely similar ones are in different conformational substates. Flash photolysis experiments on CO-liganded myoglobin yielded the first experimental support of this view (1). Consequently, the atoms in different molecules have a mean-square displacement, $\langle x^2 \rangle$, from the mean position as determined from the ensemble average. X-ray structure analysis has provided $\langle x^2 \rangle$ values of all nonhydrogen atoms of several proteins—e.g., lysozyme (2), trypsinogen (3), and myoglobin (4, 5). However, this information can be obtained also from computer simulations of protein dynamics (6–8) or from normal mode analysis (9, 10). (*ii*) Flexible protein molecules can move from one conformational substate into another. Therefore, protein dynamics also must be characterized by the transfer rates between the conformational substates.

Protein-dynamics simulations (6–8) as well as normal-mode analysis (9, 10) yield a frequency spectrum of the protein motion. The majority of vibrational frequencies are larger than 10^{12} s^{-1}. No significant vibrational modes with frequencies below 10^{11} s^{-1} are found. However, NMR investigations yield a jump rate of about 10^1–10^6 s^{-1} for the flip of the side-chain tyrosin between the two possible positions in basic pancreatic trypsin inhibitor (11). The recombination of CO to the iron in Mb at temperatures above 160 K shows that structural relaxations with rates of 10^8 s^{-1} or lower determine the kinetics of rebinding (1). The time scale of functionally important motions is not reproduced by theoretical investigations.

In the case of iron-containing proteins, Mössbauer spectroscopy is a unique tool to determine, at the position of the iron, both the mean-square displacement and the characteristic time in which the displacement occurs. In myoglobin, Mössbauer spectroscopy labels a relaxation rate on the order of 10^8 s^{-1}. This agrees well with flash photolysis experiments but is several orders of magnitude smaller than estimates from computer simulations and normal-mode analysis.

In this paper we show that the small relaxation rates are a consequence of strongly overdamped motions in the protein. Furthermore, we give evidence that computer simulations presently applied are absolutely unable to describe the time dependence of these motions even if they predict the right $\langle x^2 \rangle$ values of the individual atoms of a molecule as determined from an ensemble average (12, 13). The present model removes inconsequences in the description of the time dependence of protein dynamics. Moreover, it explains the different temperature dependence of $\langle x^2 \rangle$ values as obtained from Mössbauer spectroscopy and from x-ray structure analysis. Thus, this model provides a consistent picture of protein dynamics and shows that the dynamics are driven by a gain in entropy.

A Model for Protein Dynamics Inferred from Investigations on Myoglobin

The iron in myoglobin is bound covalently to the four N atoms of protoporphyrin IX and to the N atom of the proximal histidine of the F helix. Protoporphyrin IX is also in close contact with the globin part of the molecule via van der Waals interactions. Therefore, motions measured at the iron nucleus label not only vibrations of the iron relative to the nearest neighbor atoms but also those within the protein entity.

The use of the ^{57}Fe nucleus in Mössbauer spectroscopy provides a characteristic time resolution (14–16). (*i*) The area of the narrow Mössbauer absorption line labels the mean-square displacement, $\langle x^2 \rangle^\gamma$, of the iron due to motions whose time scale is faster than $\tau_N = 10^{-7}$ s, the lifetime of the γ emission from the iron nucleus. (*ii*) Additional broad lines in the Mössbauer spectrum, comparable to quasi-elastic lines in neutron scattering, detect special motions with a characteristic time of about 10^{-8} s. (*iii*) Line-broadening of the narrow line is the result of slow diffusive motions.

Mössbauer spectra of deoxygenated myoglobin crystals exhibit all three features above a characteristic temperature of 200 K. Fig. 1 displays the mean-square displacements of the iron in deoxymyoglobin crystals. According to ref. 15, $\langle x^2 \rangle$ is split into two terms:

$$\langle x^2 \rangle^\gamma = \langle x_v^2 \rangle + \langle x_t^2 \rangle. \quad [1]$$

The first non-protein-specific term increases linearly with temperature and is due to lattice vibrations. The pertinent second term describes protein-specific motions that are absent below a characteristic temperature of typically 200 K. For an explanation, we start from the picture that a protein molecule can exist in a large number of conformational sub-

The publication costs of this article were defrayed in part by page charge payment. This article must therefore be hereby marked "*advertisement*" in accordance with 18 U.S.C. §1734 solely to indicate this fact.

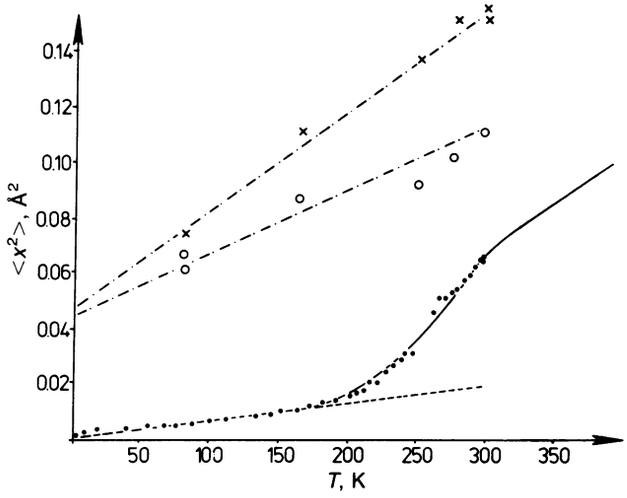

FIG. 1. Mean-square displacements obtained from x-ray structure determination and Mössbauer absorption spectroscopy as a function of temperature. Displacements of the iron: ○, $\langle x^2\rangle^x$ from x-ray data (4, 5); ●, $\langle x^2\rangle$ from Mössbauer data (15); ×, $\overline{\langle x^2\rangle}^x$ values averaged over all nonhydrogen atoms of the protein determined from x-ray structure analysis (4, 5); – – –, lattice vibrations, $\langle x_v^2\rangle$; ——, a fit of our model to the protein specific motions, $\langle x_t^2\rangle$, labeled at the iron; ·—·—, extrapolated values $\langle x^2\rangle^x$ and $\overline{\langle x^2\rangle}^x$ at $T = 0$.

states with slightly different local configurations. Let us assume for a most simple picture that the iron position is determined by only two different conformational substates of the molecule (compare Fig. 2*a*). In thermal equilibrium, the number of molecules in state 1 and state 2 depends only on the energy difference Q between the two states, assuming that there is no entropy change. There are two ways to express the transfer rates between these states. With a simple Arrhenius law, the temperature dependence of the transfer rates between states 1 and 2 is determined by the barrier heights ε and $\varepsilon - Q$ (Fig. 2*a*). In a viscous medium, the treatment according to Kramers (17) is more appropriate. Here, the transfer rates are influenced also by the physical conditions at the top of the barrier between the states. In this case the system is in a "transition state." As already discussed in ref. 18, a two-state model with $\langle x_t^2\rangle = \langle |x_1 - x_2|\rangle^2$ cannot explain quantitatively the temperature dependence of $\langle x_t^2\rangle$, although it is a starting point for more elaborate models.

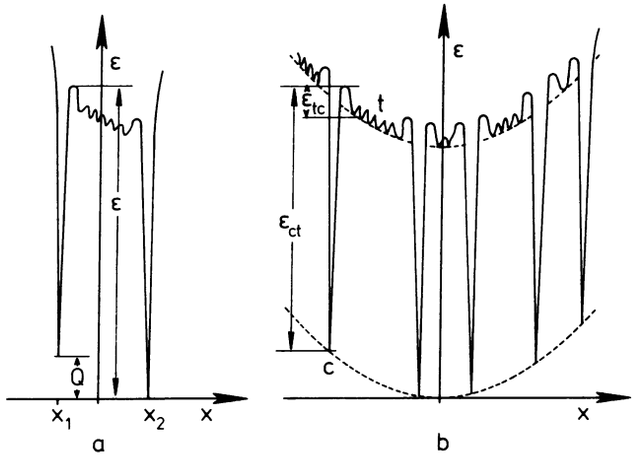

FIG. 2. A schematic representation of the potential energy as the function of one effective coordinate seen at the position of the iron. (*a*) Two-state model. Wiggles indicate the friction operating in the transition state at the top of the barrier if the transition is treated according to Kramers (17). (*b*) Generalized model taking into account a large number of conformational substates c. The parabolic envelope at the transition state (– – –) ensures a harmonic backdriving force in the transition state t. The parabolic envelope of the conformational substates accounts for a linear temperature dependence of $\langle x^2\rangle^x$. For the sake of clarity, only a few conformational substates are drawn. ε_{ct} and ε_{tc} give the potential energy to escape from a conformational substate and from the transition state, respectively. Fast fluctuations that also contribute to the friction mechanism cannot be included in this picture, although they are taken into account in the calculation. The one-dimensional representation produces the artifact not present in our model that certain parts of the transition state can be reached only by trapping in conformational substates.

A more general model has to account for a large number of conformational substates. A multisite model can be visualized as a motion in a potential given by the envelope of the sites (compare Fig. 2*b*). Before we discuss the consequences of this potential, we summarize some aspects that are partly given already elsewhere (19, 20).

Low-frequency vibrations in polypeptide chains in solution can be described by damped harmonic oscillations subjected to a random fluctuating force, $F_t(t)$, due to the Brownian motion in the solution (21). This picture has recently been applied to Mössbauer investigations (15, 16). The equation of motion for the displacement, $x_t(t)$, labeled at the position of the iron nucleus is given by

$$\ddot{x}_t + 2\,\beta_t \dot{x}_t + \omega_t^2\, x_t = F_t(t), \qquad [2]$$

where the frequency of the harmonic oscillation and the damping are given by ω_t and β_t, respectively. A numerical procedure that can account for anharmonic potentials has been pointed out by Nadler and Schulten (22). From Eq. **2**, one can calculate the spectral profile of the Mössbauer absorption and the protein-specific mean-square displacement $\langle x_t^2\rangle$. Agreement with the experiments is obtained only for a strongly overdamped motion ($\beta_t >> \omega_t$). Then the Mössbauer spectrum allows the determination of a relaxation rate related to β_t and ω_t of Eq. **2**.

$$\alpha_t = \omega_t^2/(2\beta_t). \qquad [3]$$

Although Mössbauer experiments do not provide the parameters ω_t and β_t separately, one can get an estimate of the magnitude of β_t if one takes ω_t from theoretical calculations, yielding values close to $5 \times 10^{12}\ s^{-1}$ (12). Together with $\alpha_t = 2 \times 10^8\ s^{-1}$ at room temperature, one obtains from Eq. **3** the estimate $\beta_t = 6 \times 10^{16}\ s^{-1}$. α_t^{-1} gives the average time to move over the distance $\langle x_t^2\rangle^{1/2}$.

A potential according to Fig. 2*b* can be used to visualize in part the high damping. Deep traps formed by the conformational substates and the shallow traps in the transition state are responsible for the friction.

In thermal equilibrium a constant density of conformational substates along a harmonic potential envelope of frequency ω_t gives rise to a mean-square displacement depending linearly on temperature

$$\langle x_c^2\rangle = \frac{k_B T}{m\omega_t}. \qquad [4]$$

The temperature-dependence of the protein-specific mean-square displacements, $\langle x_t^2\rangle$, obtained from Mössbauer spectroscopy is essentially determined by a probability, $p_t(T)$, to find the molecule in the transition state at the top of the barriers between conformational substates

$$\langle x_t^2\rangle = p_t(T)\,\langle x_c^2\rangle. \qquad [5]$$

The probability can be expressed by

$$p_t(T) = \{1 + \exp[\Delta G(T)/(k_B T)]\}^{-1}. \qquad [6]$$

The difference in Gibbs free energy, ΔG, between a conformational substate and the transition state can be separated as the difference of activation energies, $\Delta\varepsilon$, and entropy changes ΔS:

$$\Delta G = \Delta\varepsilon - \Delta S \cdot T = (\varepsilon_{ct} - \varepsilon_{tc}) - (S_{ct} - S_{tc})\, T, \quad [7]$$

where the indices ct and tc refer to transitions from the conformational substates to the transition state and vice versa, respectively. It has to be emphasized that Eqs. 5 and 6 contain the time threshold of Mössbauer spectroscopy as derived in ref. 20. Only processes contribute that occur faster than 10^{-7} s.

A fit of Eq. 5 to the experimentally obtained $\langle x_t^2\rangle$ values yields $p_t(T)$; in turn, $\Delta\varepsilon = 0.2 \pm 0.02$ eV and $\Delta S = 8 \times 10^{-4}$ eV/K, respectively.

It should be mentioned that our potential accounting to Fig. 2*b* uses only one type of conformational substate, although CO-flash experiments (1) reveal a distribution of well depths. It is easy to show that, in our model, $p_t(T)$ and hence α^{-1} are average values that are rather insensitive to the details of the distribution of conformational substates.

Comparison of Mean-Square Displacements Obtained from Mössbauer Spectroscopy, X-Ray Structure Investigations, and Computer Simulations

Fig. 1 gives the mean-square displacement, $\langle x^2\rangle^x$, of the iron in metmyoglobin obtained from x-ray structure analysis. The data at 300 K, 275 K, and 250 K are taken from ref. 4. At 80 K we give the value of ref. 5 and a value calculated with different constraints. The variation of these two values shows the regime in which the absolute value can be manipulated [165 K values are from our own experiments (to be published elsewhere)]. The $\langle x^2\rangle^x$ values averaged over all atoms of the molecule using the conventional overall B-factor of x-ray structure analysis are included in Fig. 1.

Mean-square displacements derived from x-ray structure determination contain the following contributions

$$\langle x^2\rangle^x = \langle x_v^2\rangle + \langle x_{ct}^2\rangle + \langle x_{qd}^2\rangle + \langle x_{sd}^2\rangle. \quad [8]$$

In comparison to Mössbauer spectroscopy, $\langle x_t^2\rangle$ in Eq. 1 has to be replaced by $\langle x_{ct}^2\rangle$ since x-ray structure analysis cannot discriminate between the distribution of conformational substates, $\langle x_c^2\rangle$, and the fluctuations between them. In comparison of Mössbauer and x-ray mean-square displacements, the following inequality should hold

$$\langle x_t^2\rangle \leq \langle x_{ct}^2\rangle. \quad [9]$$

Very slow processes are considered by $\langle x_{qd}^2\rangle$. They do not contribute to the Lamb Mössbauer factor but reveal themselves in the Mössbauer spectrum by a line broadening. Static disorder accounted for by $\langle x_{sd}^2\rangle$ does not influence the Mössbauer spectrum (4, 5, 23).

We now can compare the temperature dependence of the $\langle x^2\rangle$ values of iron as measured by Mössbauer spectroscopy and x-ray structure analysis. As seen from Fig. 1, within the present experimental accuracy, a linear temperature dependence of $\langle x^2\rangle^x$ is obtained. It is consistent with a parabolic overall shape of the potential shown in Fig. 2 and justifies the use of a harmonic backdriving force in Eq. 2. In going from physiological conditions to lower temperatures, the probability to find a molecule in a transition state diminishes. Consequently, the distance $\langle x_t^2\rangle^{1/2}$ explored in the time α_t^{-1} is reduced. The stronger decreases of $\langle x^2\rangle^\gamma$ with temperature as compared with $\langle x^2\rangle^x$ shows that the thermal population of conformational substates includes processes with characteristic times longer than τ_N. Even well below 200 K, where $p_t(T)$ is practically zero and $\langle x_t^2\rangle$ becomes immeasurably small, thermal equilibrium of the population of conformational substates is reached during the time needed for x-ray investigations.

It should be emphasized that a potential as shown in Fig. 2*b* but with only one conformational substate also can explain the temperature dependence of $\langle x_t^2\rangle$ obtained from Mössbauer spectroscopy. However, it would not explain the temperature dependence of the $\langle x^2\rangle^x$ values from x-ray data. Moreover, it would be in contradiction to the data obtained from flash photolysis experiments on CO myoglobin (1).

Not only $\langle x^2\rangle^x$ at the position of the iron but also the overall value $\langle x^2\rangle^x$, which averages over all atoms of the molecule, shows a linear dependence on temperature. The $\langle x^2\rangle^R$ values obtained from Rayleigh scattering of Mössbauer radiation (24), which averages over all atoms in the molecule and detects only motions faster 10^{-7} s, have a similar temperature dependence as the $\langle x^2\rangle$ values labeled at the position of the iron. Does this mean that the potential according to Fig. 2*b* is typical for all positions in myoglobin? This would be in contradiction to the result of refs. 4 and 5 in which nonlinear temperature dependences of $\langle x^2\rangle^x$ were found for a large number of residues. At present this question cannot be answered definitely. Accurate x-ray investigations at different temperatures are still necessary.

An additive temperature-independent contribution $\langle x^2\rangle^x - \langle x^2\rangle^\gamma = 0.045$ Å^2 obtained at 300 K and from a linear extrapolation to 0 K reflects a displacement common to all atoms of the molecule.

The $\langle x^2\rangle^x$ value and the $\langle x^2\rangle^\gamma$ value defined by Eqs. 1 and 8 can be extrapolated to temperatures above 300 K. There they both exhibit a linear temperature dependence with roughly the same slope (Fig. 1). The agreement in the slope tells us that now the temperature is high enough to explore all accessible parts of the adiabatic potential (Fig. 2*b*) within the life-time 10^{-7} s of the Mössbauer nucleus.

Computer simulations yield the mean-square displacements of all atoms in a protein molecule and the characteristic rates that are required to explore the various parts of the coordinate space available. Protein-dynamics simulations require knowledge about all details of the potential energy between the various parts of the protein molecule. After reaching thermal equilibrium, the simulation extends typically over 5–50 ps (6–8).

In the harmonic approximation, normal mode analysis and simulation of protein dynamics are equivalent, and the mean-square displacement depends strictly linearly on temperature. Both methods consider one single molecule. To obtain the mean-square displacements, a time average is performed. $\langle x^2\rangle$ values obtained from a time average can then be compared with $\langle x^2\rangle$ values determined by x-ray structure analysis, which employs an ensemble average. Reasonably good agreement is obtained (10, 12).

In statistical mechanics, an ensemble average is equivalent to a time average only if an infinite number of molecules is compared with the time average of a single molecule over an infinite sampling time; 10^{16} molecules in a crystal is a virtually infinite number. An infinite sampling time means in our example that the time is sufficiently long that the molecule can explore the available phase space. For the one-dimensional potential displayed in Fig. 2*b*, x values between a certain limit that determines $\langle x^2\rangle^{1/2}$ have to be reached within the sampling times. The reasonable agreement between computer simulations and x-ray structure determinations shows that the potential used for the computer simulations can indeed be explored within 50 ps. Therefore, longer sampling times will not produce relevant new features.

The Time Scale of Protein Dynamics

Vibrational frequencies of small molecules can be as large as 10^{15} s^{-1}. This is also an upper limit for proteins. Low-frequency vibrations play an important role in polypeptide chains (21). A chain of 10 C atoms shows frequencies as low as 7×10^{12} s^{-1}, while a chain of 94 C atoms yields frequencies as low as 7×10^{11} s^{-1}. Computer simulations (6–8) as well as normal-mode analysis (9, 10) provide frequencies in the same order of magnitude as the lower limit.

Photo-flash experiments (1), however, prove the physiological importance of motions at much lower rates. Mössbauer experiments display important contributions to protein dynamics with rates of the order of 10^8 s^{-1}. Thus, theoretical descriptions and experimental results show a discrepancy of several orders of magnitude of the time scale of protein dynamics in the low-frequency regime. The lack of the slow-relaxing components in present protein-dynamics simulations can be explained without any detailed analysis.

Mössbauer experiments show that the slow relaxation rates are due to highly overdamped modes of motions. This is reflected by a large frictional coefficient β_t. In the potential shown in Fig. 2*b*, the adiabatic parts of the friction are indicated by small wiggles in the transition state as well as by the density and the well depths of the conformational substates. The time necessary to explore this potential is $\alpha^{-1} \approx 10^{-8}$ s. Such a potential definitely cannot be explored within 50 ps. Neglecting the surrounding medium of the protein molecule in computer calculations smoothes the potentials in a way that essentially underestimates the damping. Such potentials are closer to the potential envelope shown in Fig. 2*b* than to the full potential itself. An artificially lower damping allows the system to explore the potential much faster. Hence, a short sampling time can provide a correct time average. However, this does not prove that the simulations give also the correct time dependence of protein dynamics. A potential yielding good $\langle x^2 \rangle$ values after a sampling time of 50 ps cannot contain the real damping as found by the experiments.

Note that, in a harmonic potential, the ensemble-averaged mean-square displacement according to Eq. 4 does not depend on the frictional coefficient (25). We also expect this to be valid for anharmonic potentials, although the temperature dependence will differ. Therefore, ensemble-averaged mean-square displacements as obtained by x-ray structure analysis cannot provide a full picture of protein dynamics.

Comparing the results from x-ray structure analysis and Mössbauer spectroscopy, one can attribute a time scale to the processes that are responsible for the mean-square displacement of the iron in myoglobin. At room temperature $\approx$18% comes from motions with $\tau_c < 10^{-9}$ s ($\langle x_v^2 \rangle$), 42% from motions with $\tau_c \approx 3 \times 10^{-9}$ s ($\langle x_t^2 \rangle$), 14% from motions with $\tau_c \approx 10^{-7}$ s, and the rest (i.e., 26%) from motions significantly slower than 10^{-7} s.

The Driving Force of Protein Dynamics

Chemical processes are driven by lowering the Gibbs free energy. Processes that essentially run in the direction of lower enthalpy are energy driven, whereas processes that move towards higher entropy are entropy driven. Enthalpy and entropy changes can be obtained from Mössbauer experiments by Eqs. 6 and 7 for the jump of a molecule from a conformational substate into the transition state. The enthalpy change of $\Delta\varepsilon = 0.2$ eV, which corresponds to a temperature difference of 2300 K, clearly favors the freezing of a molecule in a conformational substate even at room temperature. However, with increasing temperature the gain in entropy ($\Delta S = 8 \times 10^{-4}$ eV/K) in the transition state becomes more and more important. At room temperature the entropy change ΔS overcompensates the enthalpy change $\Delta\varepsilon$. The high entropy of the transition state drives the protein out of the conformational substate. Our results show that the phase-space volume of the transition state is 10^4 times larger than the volume of the conformational substates.

Conclusions

The detailed understanding of the function of a protein starts with the x-ray structure determination. However, the average static picture obtained this way has to be refined. Conformational substates were introduced to account for slightly different molecule structures with similar energies.

Our investigation shows that protein dynamics are mainly determined by the physical process of surmounting the barriers between conformational substates. The tops of the barriers, called as usual transition states, are rather extended in the phase space and involve a large entropy. By definition the transition state links the conformational substates. Therefore, a high probability to reach the transition state makes the protein rather flexible. Driven by an entropy gain, the molecule has a high probability to be in the transition state at physiological temperatures.

Conformational substates and the transition states constitute a potential that gives rise to an overdamped Brownian diffusion in a restricted space. The full potential is explored in about 10^{-8} s. Computer simulations that average over a sampling time of 5×10^{-11} s only are incapable of exploring such a potential. Therefore, they necessarily fail in a description of protein dynamics in the low-relaxation-rate regime.

We gratefully acknowledge the continuous support by S. F. Fischer and R. L. Mössbauer and valuable discussions with H. Frauenfelder. We thank L. Reinisch for critical reading of the manuscript. This work was supported by the Deutsche Forschungsgemeinschaft (Pa 178/9/2 and SFB 143/C2) and the Bundesministerium für Forschung und Technologie.

1. Austin, R. H., Beeson, K. W., Eisenstein, L., Frauenfelder, H. & Gunsalus, I. C. (1975) *Biochemistry* **14,** 5355–5373.
2. Artymiuk, P. J., Blake, C. C. F., Grace, D. E. P., Oatley, S. J., Phillips, D. C. & Sternberg, M. J. E. (1978) *Nature (London)* **280,** 563–568.
3. Walter, J., Steigemann, W., Singh, T. P., Bartunik, H., Bode, W. & Huber, R. (1982) *Acta Crystallogr. Sect. B* **38,** 1462–1472.
4. Frauenfelder, H., Petsko, G. A. & Tsernoglou, D. (1979) *Nature (London)* **280,** 558–563.
5. Hartmann, H., Parak, F., Steigemann, W., Petsko, G. A., Ringe Ponzi, D. & Frauenfelder, H. (1982) *Proc. Natl. Acad. Sci. USA* **79,** 4967–4971.
6. McCammon, J. A. & Karplus, M. (1980) *Annu. Rev. Phys. Chem.* **31,** 29–45.
7. Karplus, M. & McCammon, J. A. (1981) *Crit. Rev. Biochem.* **9,** 293–349.
8. Levitt, M. (1982) *Annu. Rev. Biophys. Bioeng.* **11,** 251–271.
9. Go, N., Noguti, T. & Nishikawa, T. (1983) *Proc. Natl. Acad. Sci. USA* **80,** 3696–3700.
10. Levitt, M., Sander, C. & Stern, P. S. (1984) *Int. J. Quant. Chem. Quant. Biol. Symp.* **10,** in press.
11. Wagner, G., DeMarco, A. & Wüthrich, K. (1976) *Biophys. Struct. Mech.* **2,** 139–158.
12. Levy, R. M., Perahia, D. & Karplus, M. (1982) *Proc. Natl. Acad. Sci. USA* **79,** 1346–1350.
13. van Gunsteren, W. F., Berendsen, H. J. C., Hermans, J., Hol, W. G. J. & Postma, J. P. M. (1983) *Proc. Natl. Acad. Sci. USA* **80,** 4315–4319.
14. Mössbauer, R. L. (1984) in *Proceedings of the International Conference on the Applications of the Mössbauer Effect,* Alma-Ata, U.S.S.R., ed. Goldanskii, V. I. (Gordon & Breach, New York), in press.
15. Parak, F., Knapp, E. W. & Kucheida, D. (1982) *J. Mol. Biol.* **161,** 177–194.
16. Bauminger, E. R., Cohen, S. G., Nowik, I., Ofer, S. & Yariv, J. (1983) *Proc. Natl. Acad. Sci. USA* **80,** 736–740.

17. Kramers, H. A. (1940) *Physica* **7**, 284–305.
18. Parak, F., Frolov, E. N., Mössbauer, R. L. & Goldanskii, V. I. (1981) *J. Mol. Biol.* **145**, 825–833.
19. Knapp, E. W., Fischer, S. F. & Parak, F. (1982) *J. Phys. Chem.* **86**, 5042–5047.
20. Knapp, E. W., Fischer, S. F. & Parak, F. (1983) *J. Chem. Phys.* **78**, 4701–4711.
21. Peticolas, W. L. (1979) *Methods Enzymol.* **61**, 425–458.
22. Nadler, W. & Schulten, K. (1983) *Phys. Rev. Lett.* **57**, 1712–1715.
23. Parak, F. & Formanek, H. (1971) *Acta Crystallogr. Sect. A* **27**, 573–578.
24. Krupyjanskii, Yu., Parak, F., Goldanskii, V. I., Mössbauer, R. L., Gaubmann, E. E., Engelmann, H. & Suzdalev, I. P. (1982) *Z. Naturforsch. C* **37**, 57–62.
25. Chandrasekhar, S. (1943) *Rev. Mod. Phys.* **15**, 1–89.